Dark Galaxies and Lost Baryons
Proceedings IAU Symposium No. 244, 2007
J. I. Davies & M. J. Disney, eds.

doi:10.1017/S1743921307013993

Strong Gravitational Lensing: Bright Galaxies & Lost Dark-Matter

L. V. E. Koopmans[1]

[1]Kapteyn Astronomical Institute, University of Groningen,
P.O.Box 800, 9700 AV Groningen, The Netherlands

Abstract. Gravitational lensing and stellar dynamics provide two complementary methods to probe the smooth and clumpy stellar and dark-matter mass distribution in early-type galaxies, currently already over a range of two orders of magnitude in virial mass, more than ten orders of magnidude in dynamic mass range in each galaxy (i.e. from stars, CDM substructure to massive dark-matter halos), over 0–1 in redshift, and a range of 0–100 effective radii. This makes their unification a powerful new tool in the study of the formation, structure and evolution of these massive systems. I review recent results that we obtained, based on gravitational lens systems from the *Sloan Lens ACS Survey* (SLACS), and outline some ongoing and future work.

Keywords. gravitational lensing – Galaxy: kinematics and dynamics

1. Introduction

Understanding the formation, evolution and structure of massive early-type (E/S0) galaxies is a critical test of the hierarchical galaxy formation scenario and how dark and baryonic matter interact in a process that leads to a relatively stable and uniform "end-product", that exhibits strong scaling relations (e.g. FP). Despite tremendous progress, details about these formation processes are still poorly understood. This is largely due to a total lack of information about their structural redshift evolution and our inability to separate the contribution of stellar and dark matter, or even to assess whether the systems contain dark matter at all. Gravitational lensing and stellar dynamics provide two complementary methods (e.g. Koopmans & Treu 2003; Treu & Koopmans 2004), based solely on gravity, to probe these inner regions to redshifts of $z \approx 1$ (look-back times of 8 Gyrs) with present-day ground and space-based instruments. Their combination breaks some of the most formidable degeneracies in both methods (i.e. the mass-sheet and mass-anisotropy degeneracies) that have prohibited their mass structure to be studied beyond the local Universe (e.g. Barnabè & Koopmans 2007; Vegetti & Koopmans 2007, in prep.)

2. The Basics

In this section, I will introduce the basic idea how the combination of gravitational lensing and stellar dynamics allows one to assess the effective density slope inside the Einstein radius of lens galaxies and how grid-based techniques can be used to determine two-dimensional mass maps of lens galaxies.

2.1. *Gravitational Lensing & Stellar Dynamics*

Assuming that the lens-galaxy under consideration is fully spherical and lenses a source in to a perfect Einstein ring, one can derive the mass enclosed by the Einstein ring $M_{\rm E}$ to a few percent accuracy from the Einstein radius $R_{\rm E}$ and the lens and source redshifts

$$M_{\rm E} = \pi \Sigma_{\rm crit} R_{\rm E}^2, \tag{2.1}$$

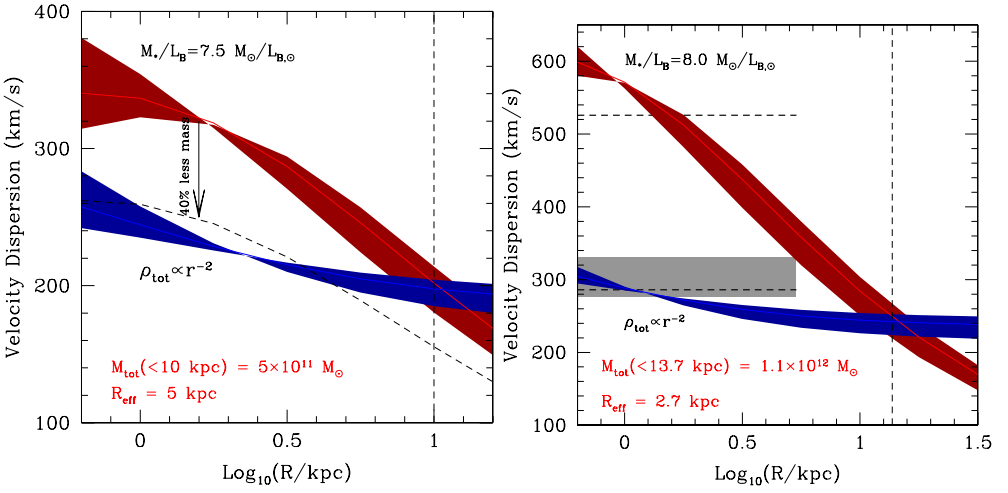

Figure 1. *Left*: Shown is a mock lens system with known mass $M_{\rm E}$, inside $R_{\rm E}$, and effective radius. The stellar velocity dispersion profiles are shown for a constant M/L model (top curve in red) and an isothermal density profile (lower curve in blue). The widths of the curves indicate a range in orbital anisotropies. Note that a single measurement of a stellar velocity dispersions of such a system would enable us to distinguish between these models (or intermediate cases), if the lens mass is know. Contrary, if the lens mass is not know, the top curve can be overlaid on the lower curve by decreasing the mass of the galaxy by some 40% and modifying the anisotropy slightly: *the mass-anisotropy degeneracy*. Hence the addition of lensing information breaks this degeneracy to a large extend. *Right:* Idem for the observed system MG2016+112, where the grey box indicates the observed luminosity weighted stellar velocity dispersions and the dashed lines indicate the two inferred dispersion for the constant M/L and isothermal mass models (see Koopmans & Treu 2002; Treu & Koopmans 2002).

where $\Sigma_{\rm crit}$ is the critical surface density for lensing to occur (e.g. Schneider, Ehlers & Falco 1992). Under these assumptions of symmetry, this projected mass is *independent* from the density profile of the galaxy, although this even holds to good precision for non-spherical asymmetric systems (see e.g. Kochanek 1991). Assuming that the total and stellar density profiles can be approximated by power-law profiles, $\rho_* \propto r^{-\delta}$ and $\rho_{\rm t} \propto r^{-\gamma}$, respectively, solving the spherical Jeans equations yields

$$\boxed{\langle \sigma^2_{||} \rangle (\leqslant R_{\rm A}) = \frac{1}{\pi} \left[\frac{G M_{\rm E}}{R_{\rm E}} \right] f(\gamma, \delta, \beta) \times \left(\frac{R_{\rm A}}{R_{\rm E}} \right)^{2-\gamma}} \tag{2.2}$$

for the luminosity weighted stellar velocity dispersion inside an aperture with radius $R_{\rm A}$, with

$$f(\gamma, \delta, \beta) = 2\sqrt{\pi} \left(\frac{\delta - 3}{(\xi - 3)(\xi - 2\beta)} \right) \times \left\{ \frac{\Gamma[(\xi - 1)/2]}{\Gamma[\xi/2]} - \beta \frac{\Gamma[(\xi + 1)/2]}{\Gamma[(\xi + 2)/2]} \right\} \times \left\{ \frac{\Gamma[\delta/2]\Gamma[\gamma/2]}{\Gamma[(\delta - 1)/2]\Gamma[(\gamma - 1)/2)]} \right\}, \tag{2.3}$$

where $\xi = \gamma + \delta - 2$ and β is the (constant) orbital anisotropy parameter (Binney & Tremaine 1987). Note that under the assumption of $\gamma = \xi = \delta = 2$ and $\beta = 0$ the simple SIS result is recovered (i.e. $f = 1$). Given this result, one can calculate (assuming uncorrelated errors and negligible errors on δ and β) the fractional error on

https://doi.org/10.1017/S1743921307013993 Published online by Cambridge University Press

the logarithmic density slope of the lens galaxy

$$\left\langle \delta_\gamma^2 \right\rangle = \alpha_g^{-2} \left\{ \left\langle \delta_{M_{\rm E}}^2 \right\rangle + 4 \left\langle \delta_{\sigma_{||}}^2 \right\rangle \right\}, \tag{2.4}$$

with

$$\alpha_g \equiv \frac{1}{2} \left(\frac{\partial \log f}{\partial \log \gamma} - \gamma \log \left[\frac{R_{\rm A}}{R_{\rm E}} \right] \right) \sim \text{few},$$

where $\delta_{...}$ indicate the fractional errors on each respective quantity. Given that the mass of the galaxy in general can be determined much more accurately than the stellar velocity dispersion, a good rule of thumbs is

$$\boxed{\delta_\gamma \sim \delta_{\sigma_{||}}}. \tag{2.5}$$

Typicially errors on measured stellar velocity dispersions of $> L_*$ galaxies out to $z \approx 1$ are $\sim$5$-$10% in one night of observing time with present-day 8–10 m class telescopes. One might therefore expect comparable errors on their inferred density slopes. This has indeed been confirmed by observations of the lens system MG2016+112 at z = 1.004 (e.g. Koopmans & Treu 2002; Treu & Koopmans 2002). The above rule-of-thumb also holds in more complex situations and should be considered conservative, because the constraints set on the density slope by the differentially magnified structure of the lensed images has not been accounted for in this estimate. To do this, a more sophisticated analysis is asked for, which will be discussed below.

2.2. *Non-parametric Lensing*

The simplest way to constrain the mass distribution of a lens galaxy is to model only the centroids of the lensed images, assuming they are associated with the centroid of the unlensed source. This leads to a set of coupled non-linear parametric equations, which can be solved using standard techniques (e.g. Keeton 2001). The situation becomes more difficult if the lensed images have complex structure that can not on-to-one be associated in each of the lensed images (see Figure4). To approach this, Warren & Dye (2003) developed a semi-linear inversion technique that allows one to determine the structure of the unlensed source that minimizes a likelihood penalty function. This function is further minimized with respect to the parameters that determine the properties of a parametric lens potential. This way *all* information is used to constrain the mass distribution of the lens galaxy. Koopmans (2005) and Suyu *et al.* (2006) further enhanced this idea by incorporating a linearized correction of the lens potential (Blandford *et al.* 2001), making the method fully non-parametric both for the source and the lens potential. The idea is the following:

(1) Suppose we have a guess of the source model $s_i(\vec{y})$ and potential model $\psi_i(\vec{x})$ then

$$s_i(\vec{x} - \vec{\nabla}\psi_i(\vec{x})) = d(\vec{x}) + \delta d(\vec{x})$$

with $\delta d(\vec{x})$ the mismatch between data and model.

(2) The potential can then be corrected such that

$$s_i(\vec{x} - \vec{\nabla}[\psi_i(\vec{x}) + \delta\psi(\vec{x})]) = d(\vec{x})$$

Assuming the source model is correct.

(3) Linearising this equation yields

$$\boxed{\delta d(\vec{x}) = -\vec{\nabla}_y s_i(\vec{y}) \cdot \vec{\nabla}_x \delta\psi(\vec{x})}$$

https://doi.org/10.1017/S1743921307013993 Published online by Cambridge University Press

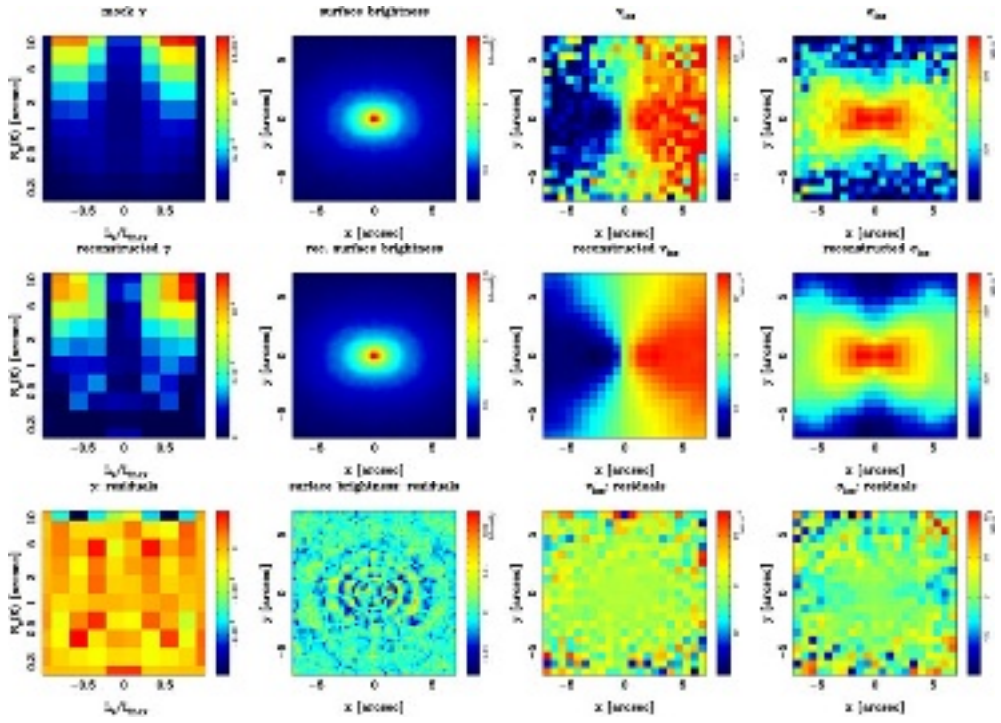

Figure 2. *Top row:* From left to right are show the (rescale) phase space distribution function, galaxy surface brightness, l.o.s. velocity and velocity dispersions, respectively, for a mock lens system (the lensing constraints are omitted, but see BK07). The *middle row* show the best reconstruction, and the *bottom row* shows the residuals. Note the excellent reconstruction.

.

(4) The above equation is linear and can easily be solved (Koopmans 2005). We then set

$$\psi_{i+1}(\vec{x}) = \psi_i(\vec{x}) + \delta\psi(\vec{x})$$

providing an updated potential model.

(5) We then have

$$s_{i+1}(\vec{x} - \vec{\nabla}\psi_{i+1}(\vec{x})) = d(\vec{x}) + \delta\tilde{d}(\vec{x})$$

which can be solved exactly.

(6) We then return to –2– and iterate until

$$\delta d(\vec{x}) \approx 0$$

i.e. convergence in a χ^2 sense. In the next section, I will outline how this general scheme can be implemented using a grid to describe the source and lens potential.

3. Grid-based Gravitational Lensing & Stellar Dynamics

To objectively model the extended imaging and 2D stellar kinematic data from galaxy-scale lens systems, and extract from it the *maximum* amount information about the mass distribution of the lens galaxies, traditional modeling techniques based on point or line descriptions of the source, as discussed in the previous section, are therefore no longer sufficient. The number of lens systems with extended complex sources has increased

https://doi.org/10.1017/S1743921307013993 Published online by Cambridge University Press

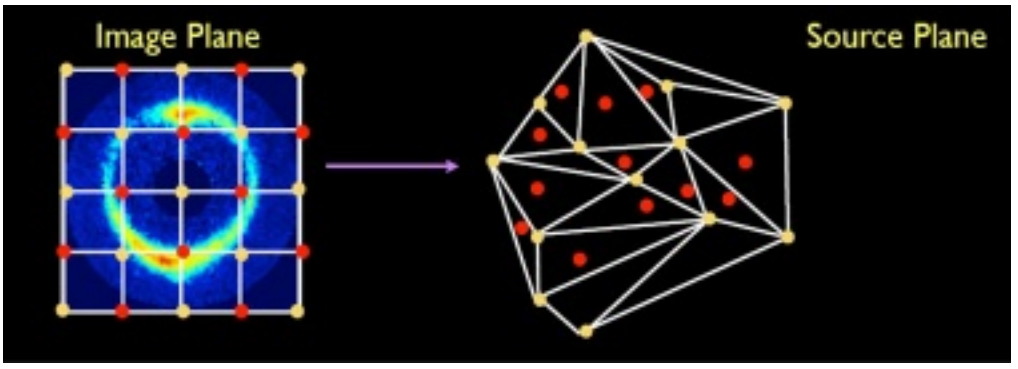

Figure 3. Outline of the adaptive grid method developed in Vegetti & Koopmans, 2007, in prep. A set of vertices in the source plane (yellow points) is defined by a set of grid-points in the image (data) plane, through the lens equation. The surface brightness at the other (red) points are determined through a predefined interpolation scheme using the yellow points. The lens operator is build from the the weights of the interpolation scheme (or are set to unicty at the vertices). This adaptive scheme ensures that (i) the source is never under-sampled, (ii) the grid adapts itself to the differential magnification caused by the lens potential and (iii) a proper accounting of the number of degrees of freedom is done in the lensing model (see Vegetti & Koopmans, 2007, in prep).

so dramatically in the last several years, that new techniques had to be developed. Recently, Barnabè & Koopmans (2007) further enhanced these lensing techniques, described above, by the inclusion of kinematic data, solving for the two-integral phase-space density models $f(E, L_z)$ in axisymmetric galaxy potentials. Even though the assumptions of axisymmetry and restriction to two-integral phase-space models still limit the models in some sense, these models capture the most relevant aspects of galactic mass model with only minor biases (e.g. see comparisons in Cappellari *et al.* 2006). To improve the dynamic range in the (regulated) solutions, more recently adaptive grid techniques have between developped (Dye & Warren 2005; Koopmans & Vegetti 2007, in prep.; Figure 3). Below I will give a brief outline of the methodology.

3.1. *Grid-based Gravitational Lensing & Stellar Dynamics*

To implement the ideas set out above in a practical manner, the easiest way to do this is to describe both the source brightness distribution and the stellar phase-space distribution function $f(E, L_z)$ on a regular grid. It turns out (Barnabè & Koopmans 2007) that this can be formally written as a coupled set of linear equation (for fixed non-linear parameters of the lens potential):

$$\vec{d} = \mathbf{L}(\vec{\eta})\vec{s} + \vec{n}_d \tag{3.1}$$

and

$$\vec{p} = \mathbf{Q}(\vec{\eta})\vec{\gamma} + \vec{n}_p, \tag{3.2}$$

for the lensing and dynamical data-sets respectively. These equations can be regularized and solved using standard techniques, resulting in the "best-fit" solutions for the source surface brightness distribution and the stellar phase-space density, *given a set of non-linear parameters* $\vec{\eta}$ *that describe the lens potential*. Using non-linear optimization techniques this resulting penalty as function of $\vec{\eta}$ can be solved to find the maximum likelihood solution of the lens-potential parameters. Figure 2 shows an example where this techniques has been applied to a simulated lens system (see BK07). Note the excellent reconstruction under realistic circumstances. In BK07 it is also shown that the combination

https://doi.org/10.1017/S1743921307013993 Published online by Cambridge University Press

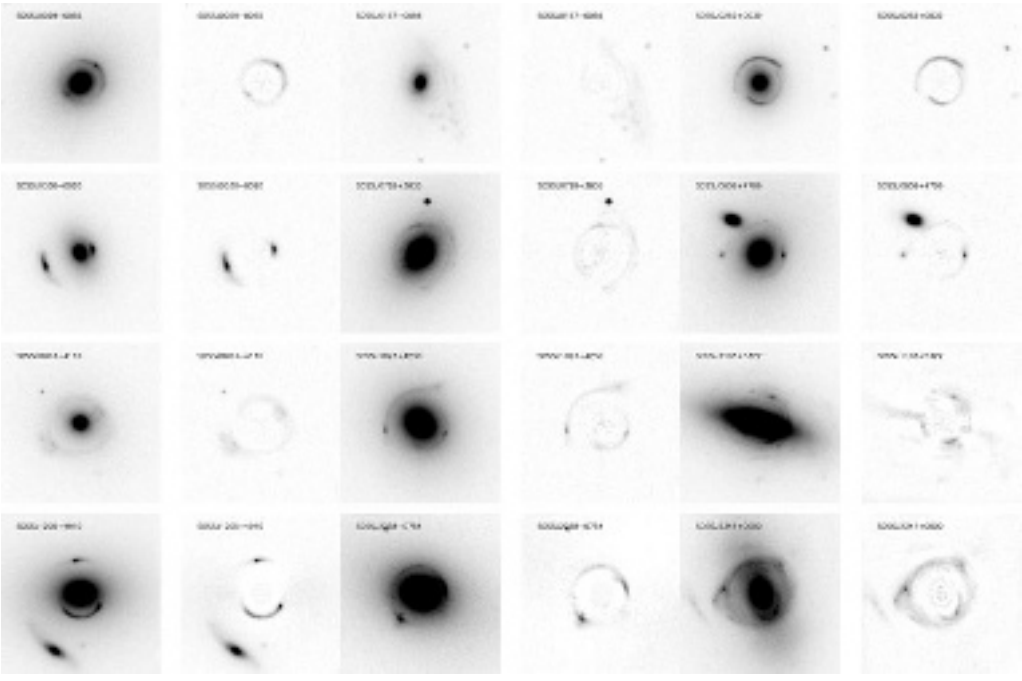

Figure 4. Gallery of a subsample of SLACS lens systems (from Gavazzi *et al.* 2007).

of these two techniques, lensing and dynamics, not only can break the mass-anisotropy degeneracy, but also break the oblateness-inclination degeneracy, which inhibits analyzes of early-type galaxies (e.g. Capellari *et al.* 2006, 2007). This new technique is currently being applied to lens systems with available HST and 2D kinematic data (from VLT-IFU observations).

4. The Sloan Lens ACS Survey

The Sloan Lens ACS Survey (SLACS; Bolton *et al.* 2006; Treu et al. 2006; Koopmans *et al.* 2006; Gavazzi *et al.* 2007; papers I-IV hereafter) has spectroscopically selected lens candidates from the SDSS (see paper I) – based on the detection of emission-lines inside a 3 arcsec diameter optical fibre – at a redshift large than that of foreground early-type galaxies. The alignment of a background source and massive foreground galaxy (the stellar velocity dispersion is know from the SDSS spectra), within a radius of 1.5 arcsec, make such systems excellent gravitational lens candidates. Follow-up with HST (V, I and H-band) has resulted in the discovery of nearly one hundred new lens systems (some shown in Figure 4), which are further being follow-up with the VLT/Keck to obtain improved spectra for kinematic analyzes (Czoske *et al.* 2007, in prep). This makes SLACS the most successful galaxy-scale lens survey to date. More details can be found in papers I-IV. The deep ACS/WFPC2 multi-color observation, combined with extended stellar kinematic data from VLT IFU and Keck long-slit observations allow a large range of studies of these massive galaxies out to a redshift range of $\sim$0.4. In combination with previous studies at higher redshifts (the LSD Survey; Koopmans & Treu 2003; Treu & Koopmans 2004) allows this redshift range to be extended to $z \sim 1$, although the sample becomes less homogeneous in that case. Below I will outline some selected ongoing projects.

https://doi.org/10.1017/S1743921307013993 Published online by Cambridge University Press

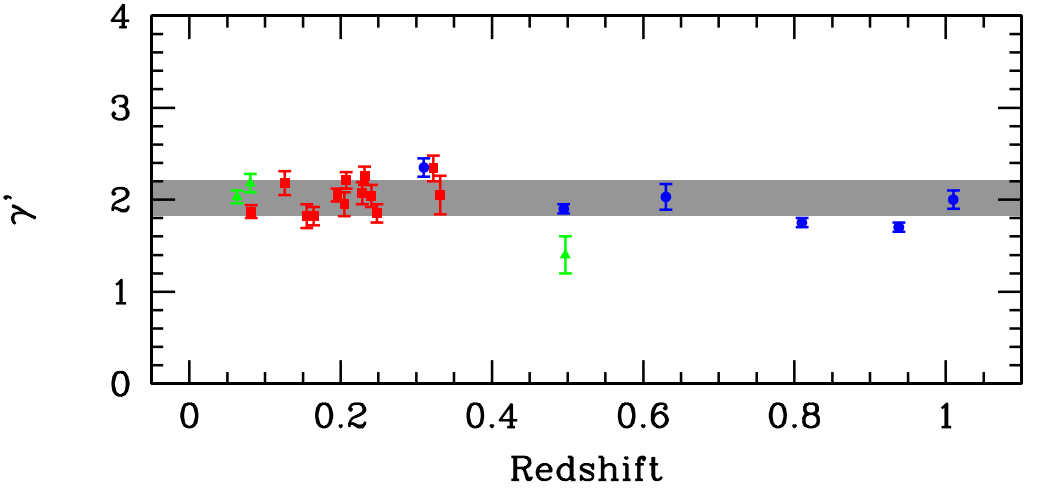

Figure 5. The logarithmic density slope of SLACS+LSD lens systems as function of redshift. Note the absence of evolution (from Koopmans *et al.* 2006).

4.1. *Inner Stellar and Dark-Matter Density Profiles*

One of the main goals of the SLACS survey is to quantify the average and intrinsic spread of the radial density profiles of massive galaxies, as function of redshift and galaxy mass. The approach is two-fold: on the one hand, we can use only gravitational lensing to assess the effective density slope *near* the Einstein radius (e.g. Dye & Warren 2005), whereas on the other hand, we can combine this with the kinematic data to assess the effective density slope *inside* the Einstein radius. Comparison of both indicate how much the logarithmic density slope varies as function of radius within the galaxy. Initial results were presented in Koopmans *et al.* (2006) and improved analyzes are currently ongoing on a much larger sample. In particular, combined lensing and dynamical analyzes are currently underway to quantify the 3D structure of these galaxies (e.g. Czoske *et al.* 2007, in prep; BK07). One prominent result found thus far is the homogeneity of density profiles for the most massive ($> L_*$) lens galaxies, exhibiting a log. density slope of

$$\boxed{\langle \gamma' \rangle = 2.01 \pm 0.03 \quad (68\%\ \mathrm{CL})}$$

with less than 6% intrinsic spread (Koopmans *et al.* 2006). As function of redshift, including half a dozen LSD systems, no significant redshift evolution can be seen (Figure 5), suggesting that these systems are already dynamically in place at half the age of the Universe (see Koopmans *et al.* 2006 for more discussion on this point).

4.2. *Scaling Relations: the Fundamental Plane*

One of the major open issues in the study of early-type galaxies is why these galaxies populate the so called Fundamental Plane. In particular, this plane is tilted with respect to what naively is expected from the virial theorem. SLACS lens system occupy the same FP as their parent population (Treu *et al.* 2006) and show no bias other than being a more massive subsample (Bolton *et al.* 2006). Taking the latter bias into account, SLACS lenses are equivalent in their properties to a *randomly* drawn sample of galaxies from the LRG+MAIN samples from the SDSS. SLACS lens galaxies can thus been used to study the FP with an absolute minimal bias. This is purely the result of the very uniform way in which these systems were selected (based on the galaxy and not the source!). In Figure 6, the FP of SLACS galaxies is shown (middle panel). Since the mass-to-light ratio

https://doi.org/10.1017/S1743921307013993 Published online by Cambridge University Press

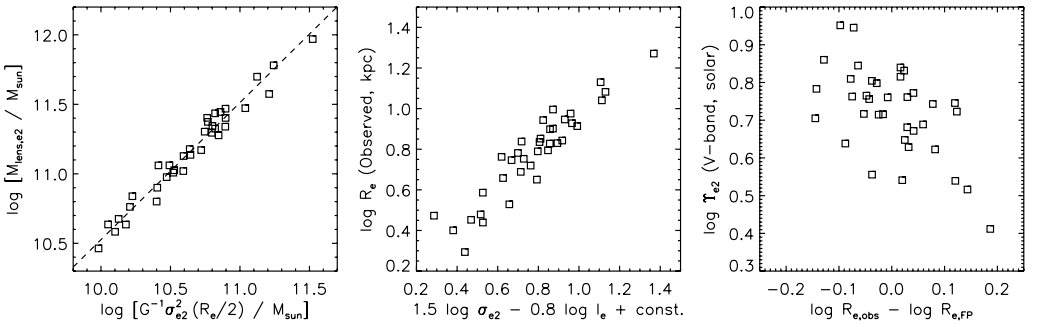

Figure 6. *Left*: relationship between lensing mass and dimensional mass within $R_e/2$. Dashed line is best fitting linear relation between these logarithmic quantities, with slope of 0.986 ± 0.034. *Center*: effective radius R_e as observed and as predicted from the best-fitting FP relationship between R_e, I_e, and σ_{e2}. *Right*: mass-to-light ratio Υ_{e2} in the V-band versus residuals about the FP relationship. (from Bolton *et al.* 2007)

of the galaxy can be determined accurately from the observed HST data and lens model, lenses provide a unique way of checking whether residuals from the FP correlate with total M/L. Figure 6 shows that this is indeed the case (right panel) and that the total M/L variations is one of the major causes of scatter in the FP. Furthermore, the galaxies closely follow the virial plane (left panel Figure 6), which is expected if these galaxies are all close to isothermal (as shown in the previous section). Hence the conclusion is that the tilt in the FP results from replacing surface density with surface brightness, under the assumption that M/L does not vary. Inverting this argument,we conclude that the FP tilt is probably caused by a varying dark-matter fraction inside the effective radius (increasing with more massive galaxies). Stellar M/L variations are unlikely since no correlation with color or 4000Å break is found. This conclusion agrees well with that drawn from the SAURON sample (see Capelarri *et al.* 2006 for an excellent discussion) of somewhat less massive early-type galaxies. This work is further persuit in our ongoing analyzes of extended kinematic data of these systems.

4.3. *(CDM) Mass Substructure*

The abundant presence of CDM substructure around massive galaxies is a strong prediction of the CDM cosmological model (Moore *et al.* 1998). As such, its detection and quantification would be a great triumph of this model. In reality, however, it has been difficult to detect these structures, logically, because they are mostly dark (although they might have traces of gas or stars in them). Gravitational lensing provides several ways of detecting substructures. One is though so called flux-ratio anomalies (Dalal & Kochanek 2002), although degeneracies in the models and issues with the data make interpretation of some of the results difficult. A second, similar approach is to compare whether the full surface brightness distribution of highly-magnified arc and Einstein rings show evidence for substructure (Koopmans 2005). Einstein rings are particularly sensitive to small potential perturbations, because of their near-degenerate Fermat potential. Any perturbation will lead to a complete re-mapping of the source on to the image plane. Using grid-based modeling techniques the effect of substructure can be extracted from the lensed images and separated from the structure of the source, leading to a 2D mass map inside the annulus around the lensed images. If present, substructure with $M_{\rm vir} > 10^7$ solar mass can be detected this way (Vegetti & Koopmans 2007, in prep). Using the SLACS lens systems and the fully-adaptive grid-based technique discussed above, limits on the presence (or absence) of CDM can soon be set.

https://doi.org/10.1017/S1743921307013993 Published online by Cambridge University Press

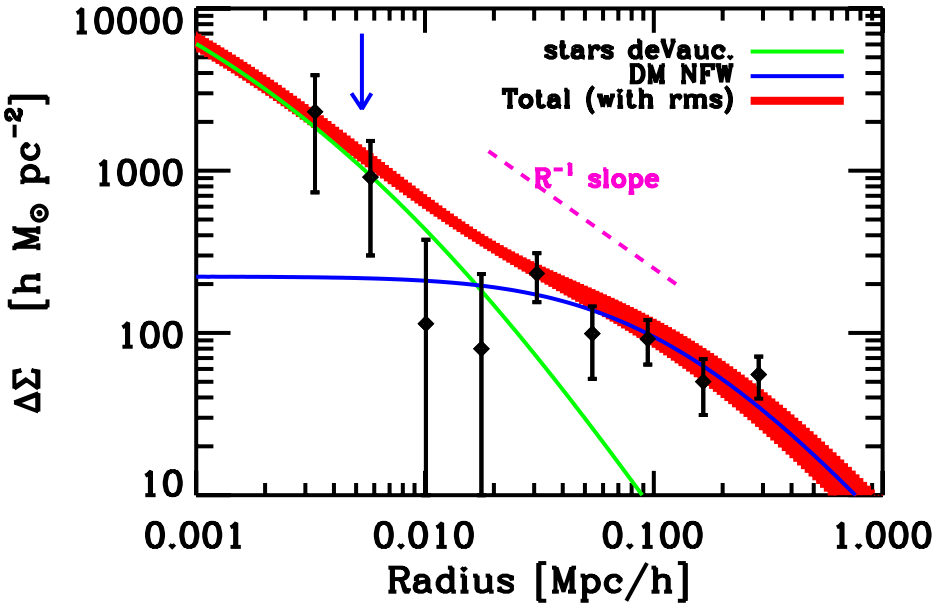

Figure 7. Shear profile of SLACS early-type galaxies for the best DM + de Vaucouleurs model. The contribution of each mass component is detailed (green and blue for stars and DM respectively). The thickness of the red curve codes for the 1σ uncertainty around the total shear profile. Uncertainties are very small below 10 kpc because of strong lensing data that cannot be shown here. (from Gavazzi *et al.* 2007)

4.4. *Extended Dark Halos & Galaxy Environment*

Going from the smallest (substructure) scales to the largest scales, the SLACS sample also allows us to study the extended DM halo around these massive galaxies. The deep HST ACS observations provide a sufficient density of background sources, such that with two dozen lens systems a weak-lensing density profile can be derived to a radius of nearly 100 effective radii (Gavazzi *et al.* 2007). Results of such an analysis are shown in Figure 7. We note here that each system is not only constraint by weak-lensing in its outer region but also by strong lensing in its inner region. Hence, the freedom of fitting density profiles, which often limits the ability to distinguish between different models, is greatly reduced. Figure 7 shows that a standard NFW DM density profile plus a stellar component (constraints by strong lensing as well!) can fit the data very well. However, simple a SIS density profile can not yet be excluded. Ongoing analysis with more data, however, should be able to settle this question soon.

5. Conclusions

Gravitational lensing – strong and weak – combined with stellar dynamics *and* the best space (HST) and ground-based (VLT/Keck) data, is for the first time allowing us to address some of the open questions regarding the structure, formation and evolution of massive early-type galaxies as function of redshift and mass. In this review I have outlined some of the basic techniques that we have developed or refined over the last several years and illustrated this when applied to lens systems discovered in the Sloan Lens ACS Survey (SLACS). With new facilities coming online in the next decades (LSST, SKA, etc.) to disover more lens systems, this techniques is expected to have a major impact on the detailed study of early-type galaxies beyond the local Universe.

https://doi.org/10.1017/S1743921307013993 Published online by Cambridge University Press

Acknowledgements

I would like to thank the organisers, in particular Jon Davies and Mike Disney, for a wonderful and eventful meeting. I would also like to thank all my colleagues in the SLACS collaboration for their joint effort in the work, the fruits of which were presented in this review. LVEK is supported in part through an NWO-VIDI program subsidy (project #639.042.505).

References

Barnabè, M., & Koopmans, L. V. E. 2007, ApJ in press, ArXiv Astrophysics e-prints, arXiv:astro-ph/0701372

Binney, J., & Tremaine, S. 1987, Princeton, NJ, Princeton University Press, 1987

Blandford, R., Surpi, G., & Kundić, T. 2001, Gravitational Lensing: Recent Progress and Future Goals, 237, 65

Bolton, A. S., Burles, S., Koopmans, L. V. E., Treu, T., & Moustakas, L. A. 2006, ApJ, 638, 703

Bolton, A. S., Burles, S., Treu, T., Koopmans, L. V. E., & Moustakas, L. A. 2007, ApJL in press, ArXiv Astrophysics e-prints, arXiv:astro-ph/0701706

Cappellari, M., *et al.* 2006, MNRAS, 366, 1126

Cappellari, M., *et al.* 2007, MNRAS, 379, 418

Dalal, N., & Kochanek, C. S. 2002, ApJ, 572, 25

Dye, S., & Warren, S. J. 2005, ApJ, 623, 31

Gavazzi, R., Treu, T., Rhodes, J. D., Koopmans, L. V. E., Bolton, A. S., Burles, S., Massey, R., & Moustakas, L. A. 2007, ApJ in press, ArXiv Astrophysics e-prints, arXiv:astro-ph/0701589

Keeton, C. R. 2001, ArXiv Astrophysics e-prints, arXiv:astro-ph/0102340

Kochanek, C. S. 1991, ApJ, 373, 354

Koopmans, L. V. E., & Treu, T. 2002, ApJL, 568, L5

Koopmans, L. V. E., & Treu, T. 2003, ApJ, 583, 606

Koopmans, L. V. E. 2005, MNRAS, 363, 1136

Koopmans, L. V. E., Treu, T., Bolton, A. S., Burles, S., & Moustakas, L. A. 2006, ApJ, 649, 599

Moore, B., Governato, F., Quinn, T., Stadel, J., & Lake, G. 1998, ApJL, 499, L5

Schneider, P., Ehlers, J., & Falco, E. E. 1992, Gravitational Lenses, Springer-Verlag Berlin Heidelberg New York. Also Astronomy and Astrophysics Library

Suyu, S. H., Marshall, P. J., Hobson, M. P., & Blandford, R. D. 2006, MNRAS, 371, 983

Treu, T., & Koopmans, L. V. E. 2002, ApJ, 575, 87

Treu, T., & Koopmans, L. V. E. 2004, ApJ, 611, 739

Treu, T., Koopmans, L. V., Bolton, A. S., Burles, S., & Moustakas, L. A. 2006, ApJ, 640, 662

Warren, S. J., & Dye, S. 2003, ApJ, 590, 673